On the Principle and Applications of Conditional Disturbance Negation

Zhiqiang Pu, Jinlin Sun, Jianqiang Yi, *Senior Member, IEEE*, and Zhiqiang Gao, *Member, IEEE*

***Abstract*—It is commonly believed that observer-based compensation is an effective way for disturbance rejection. A less talked about fact is that such disturbance rejection control technique may also degrade control performance. In this article, we present a typical cross-coupling system to reveal this problem and, more importantly, propose a new design principle of conditional disturbance negation (CDN) to eliminate its potential drawbacks of disturbance observer-based compensation. Qualitative analysis is first given for a general form of such cross-coupling systems, indicating the necessity of CDN. The analysis and control design principle of CDN is then exemplified through two applications. A numerical linear application produces abundant quantitative results through the powerful transfer function and frequency domain tools. A more complex nonlinear flexible air-breathing hypersonic vehicle application shows how conventional compensation deteriorates the couplings between rigid and flexible modes, and validates the effectiveness of CDN through comprehensive model analysis and simulation results. The proposed CDN design principle also arouses awareness of the importance of: 1) understanding the characteristics of the plant to be controlled and 2) recognizing the critical role the information plays in engineering practice.**

***Index Terms*—Conditional disturbance negation (CDN), coupling, disturbance rejection, information-centric control, observer.**

I. Introduction

ENGINEERING cybernetics is not just about control, but more so about the interaction between information and control [1], where information plays a critical role that has not been well understood yet. Generally, a control process is to achieve balance of a system by appropriately choosing, obtaining, and processing relevant information. Among abundant system information, uncertainty, and disturbance information is of great significance because, to some extent, the essence of control is to suppress the effects of uncertainty and disturbance [2], [3]. One solution to suppress the uncertainty and disturbance is the widely used error-based paradigm, where the error information is obtained through feedback and an error-based control law is designed to suppress the uncertainty and disturbance. This is a general solution but has its inherent drawback because it supposes that the uncertainty and disturbance have already caused come effects (the causal error) before the control law gets activated. A more straightforward solution is to directly obtain the uncertainty and disturbance information, which can suppress them before they affect the system. This paradigm yields the flourish development of the invariance principle [4] and the active disturbance rejection control framework [5]–[7].

In this article, we focus on a widely applied uncertainty and disturbance information constructor: the disturbance observer (DOB). Observer-based control technologies have been widely researched and applied in the last decades for rejecting inevitably existing disturbance [8]–[17]. A general case of such control schemes incorporates a two-degree-of-freedom configuration, including a controller and a DOB. The DOB-based compensation is viewed as a straightforward and cost-effective method, particularly because internal uncertainty and external disturbance may come from diverse sources and, quite often, they cannot be directly measured or are too expensive to measure. Based on this understanding, it seems that DOB-based compensation always has positive effects in control performance enhancement.

However, DOB-based control has its robustness and performance constraints [9]. Moreover, inappropriate compensation based on observed information may even cause side effect, which is rarely recognized in practice. A typical example is the compliant mechanical systems addressed in [18] and [19], where if all disturbances are compensated at the motor side, vibration at the arm side is induced because reaction torque, as a portion of the total disturbance, is canceled thus information at the arm side cannot be reflected at the motor side. In this article, we will present another typical system suffering from the side effect of DOB-based compensation. Such systems often contain multiple system states and feature severe couplings among the states and control inputs. The side effect lies in the following logic: the observer may be assumed to estimate and compensate the disturbance acting on some specific dynamics, but compensation effects may undesirably act on other dynamics due to couplings and degrade overall performance. As a result, complex cross-coupling occurs among the disturbance, the plant to be controlled, the controller, and the observer. In some special

Manuscript received August 22, 2019; revised December 1, 2019; accepted December 26, 2019. Date of publication January 22, 2020; date of current version October 15, 2021. This work was supported by the National Natural Science Foundation of China under Grant 61603383, Grant 61421004, and Grant 61403381. This article was recommended by Associate Editor Z. Wang. *(Corresponding author: Zhiqiang Pu.)*

Zhiqiang Pu, Jinlin Sun, and Jianqiang Yi are with the Institute of Automation, Chinese Academy of Sciences, Beijing 100190, China, and also with the School of Artificial Intelligence, University of Chinese Academy of Sciences, Beijing 100049, China (e-mail: zhiqiang.pu@ia.ac.cn; jinlinsun@outlook.com; jianqiang.yi@ia.ac.cn).

Zhiqiang Gao is with the Department of Electrical and Computer Engineering, Cleveland State University, Cleveland, OH 44115 USA (e-mail: z.gao@ieee.org).

Color versions of one or more figures in this article are available at https://doi.org/10.1109/TSMC.2020.2964045.

Digital Object Identifier 10.1109/TSMC.2020.2964045

cases, the observer compensation may excite some *hidden states* through the cross-coupling and finally cause overall system instability. Here, the term hidden state may be the system dynamics that is not yet well understood or assumed to be negligible thus deliberately ignored in control design. Such complex cross-coupling systems with hidden states widely exist in engineering practice. In fact, the core idea of this article originates right from our previous research [20], [21] on the control of a flexible air-breathing hypersonic vehicle (FAHV) where the flexible modes may be excited by disturbance compensation which is intended to act on rigid modes. Note that in this article the term "observer" is particularly used to represent DOB, rather than other system state observers, for expression convenience.

To eliminate potential drawbacks of the observer-based compensation, in our recent paper [22] we designed a novel disturbance characterization indicator to show whether a disturbance harms or benefits the control performance. Then we could selectively compensate the disturbance with detrimental effects. This is an early attempt for a new control design principle which does not simply feed all estimated disturbance information for compensation. Instead, it evaluates and processes the estimated information generated by a DOB first, and then *conditionally* (or selectively) feeds the processed information for disturbance negation according to characteristics of the disturbance and system dynamics. We term this new disturbance rejection principle as conditional disturbance negation (CDN). In this principle, understanding the characteristics of the plant to be controlled is important. A deep insight into system characteristics helps to understand what we can gain from an observer and how it produces side effects [23]. Then we can conditionally restrict the effect of the observer by properly processing its estimated information.

In this article, the CDN principle is systematically presented and generalized to a class of cross-coupling systems mentioned above. A general form of such systems will be given. We will conduct qualitative analysis to exhibit how conventional DOB-based compensation causes side effects and why CDN is necessary. Then we will exemplify the design of the CDN principle and validate its effectiveness through two representative examples.

The core idea of CDN is to incorporate a signal processor for adequate estimated signal processing. An intuitive implementation for such a signal processor is to design a filter following the observer. Guide for designing such a filter can be found in some previous literatures, [24] and [25], to name a few. In these papers, the filter was designed as a low-pass type and was intended to filter out high-frequency signal such as measurement noise. This is a straightforward implementation of the signal processor, but CDN brings much more possibility for observed information processing, such as the disturbance characterization indicator in [22]. Moreover, in CDN more concerns about the interaction between system dynamics and disturbance are given, yielding a more delicate result that is quite relevant to system characteristics.

To sum up, our contributions of this article mainly include.

1) Drawbacks of conventional DOB-based compensation are pointed out through a class of cross-coupling systems. This reveals the particularity of our contribution since in addition to the rare results in [18] and [19], we give another typical example to indicate potential drawbacks of DOB-based compensation.
2) The novel CDN principle is proposed as a solution to better disturbance negation for such systems. This reveals the generality of our contribution because CDN is a general design principle for a large class of systems suffering from side effects of DOB-based compensation.
3) Comparison analyses and simulations are comprehensively conducted to verify the advantages of the CDN principle over conventional disturbance compensation schemes.

We also want to heighten the critical role the information plays in engineering practice. In fact, the system characteristics can be viewed as a kind of prior or off-line information, while CDN is to conduct online information processing of the estimated disturbances. It is of great importance to construct such an information-centric control concept, especially, because there is abundant information and knowledge (appropriate collection of information) hidden in big data produced every minute nowadays [26].

This article is organized as follows. Section II gives a description of a basic form of the coupling systems discussed in this article. Based on qualitative analysis of system information flow, the design principle of CDN is proposed. Detailed analysis and control design are given through two examples next. Section III presents a numerical linear time-invariant (LTI) example. The powerful transfer function method is adopted, yielding a comprehensive quantitative analysis. Section IV gives a nonlinear application which is to design a robust control system for an FAHV. This is a more complex and practical problem, and is also the prototype where our seminal idea of this article comes from. A comprehensive model analysis is conducted to exhibit the severe cross-coupling among the plant, the controller, the observer, and external disturbance. The necessity of CDN is validated through simulation. For engineering convenience, frequency-domain language is involved in both examples. The conclusion and future work are addressed in Section V.

II. Problem Statement

Consider the following n-dimensional disturbed system:

$$\begin{cases} \dot{x}_1 = f_1(x_1, x_2, u_1, w_1) \\ \dot{x}_2 = f_2(x_1, x_2, u_1) \\ y = x_1 \end{cases} \tag{1}$$

where $x_1 \in \mathbb{R}^{n_1}$ and $x_2 \in \mathbb{R}^{n_2}$ are two system state vectors, $n_1 + n_2 = n$, $u_1 \in \mathbb{R}^m$ is an m-dimensional control input vector, y is the output vector, and $w_1 \in \mathbb{R}^p$ is a p-dimensional external disturbance vector. $f_1 \in \mathbb{R}^{n_1}$ and $f_2 \in \mathbb{R}^{n_2}$ represent corresponding linear or nonlinear system dynamics. Here, the system dynamics are divided into two groups, where x_1 represents the dynamics that is intended to be well controlled (directly or indirectly) through the control input u_1, while x_2 represents the hidden state that is deliberately ignored or not well modeled thus cannot be directly controlled. These two

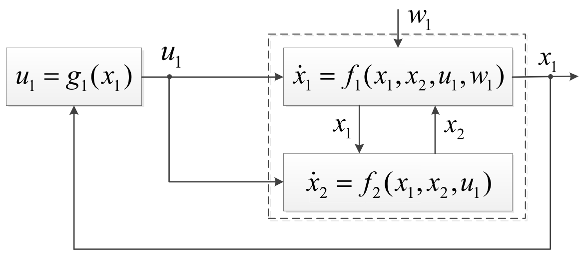

Fig. 1. System diagram for the closed-loop system without compensation.

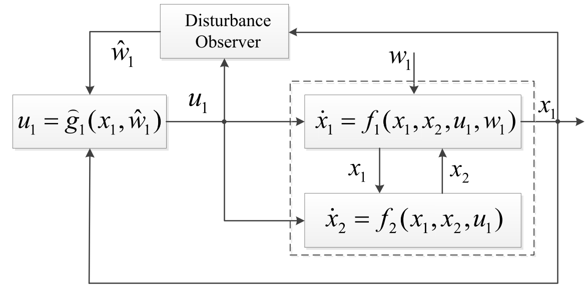

Fig. 2. System diagram for the closed-loop system with full compensation.

state groups may also be termed as two subsystems or channels in different contexts.

Assumption 1: Natural frequencies of x_1 and x_2, denoted as ω_{x1} and ω_{x2}, respectively, are far separated, $\omega_{x1} \geq 5\omega_{x2}$ or $\omega_{x2} \geq 5\omega_{x1}$, for example.

Assumption 2: The effect of w_1 on x_1 is negligible.

Assume only x_1 is measurable (since x_2 is "hidden"). Our original intent is to control the x_1 subsystem by synthesizing the control input u_1. However, since u_1 also affects the hidden dynamics x_2, coupling exists between the two subsystems through the control input and the hidden state may be undesirably excited. Next, we will illustrate how this happens through designing control schemes without and with conventional DOB-based compensation and then present the CDN scheme proposed in this article.

Remark 1: In view of Assumption 2, one could argue that it is unnecessary to incorporate such a DOB for compensation. In practice, however, a system often suffers multiple disturbances. Denote the total disturbance as $w = \{w_1, w_2\}$, where only w_1 has negligible impact on x_1, while w_2 does have great impact on x_1. However, when we design an observer, we usually consider all disturbances together. In this situation the DOB-based compensation is indeed necessary. In (1), we only consider w_1 for convenience.

A. Generic Feedback

Consider the $x_1$subsystem. A generic (state) feedback control law without DOB-based compensation is synthesized as

$$u_1 = g_1(x_1). \tag{2}$$

Here, g_1 represents any proper feedback control law that stabilizes the x_1 subsystem. A graphic interpretation of the closed-loop information flow is given as Fig. 1.

B. Full Compensation

Now, consider another control scheme: we design a DOB to obtain the estimated value $\hat{w}_1$ of the disturbance w_1. Then a feedback control law with conventional disturbance compensation is synthesized as

$$u_1 = \widehat{g}_1\left(x_1, \hat{w}_1\right). \tag{3}$$

Here, $\widehat{g}_1$ is derived from g_1 with additional cancelation of the disturbance w_1. For example, if the influence of w_1 on x_1 can be represented by $x_1 = Hw_1$, where H is some mapping or operator that specifies x_1 in terms of w_1. Then a compensation law is designed to produce a cancelation effect as $x_1 = -H\hat{w}_1$ in an additive form. This conventional compensation scheme is termed as *full compensation* since it directly (or fully) uses what the observer obtains ($\hat{w}_1$) about the disturbance (w_1) for control law synthesis. The corresponding closed-loop information flow is depicted as Fig. 2. Note that the control input u_1 explicitly contains a component $\hat{w}_1$ that is closed to w_1. Since u_1 also affects on x_2, there exists an information path through which the disturbance w_1 has an impact on the hidden dynamics x_2, while Fig. 1 does not contain such a path. This additional path, under certain conditions, may degrade the performance of the hidden dynamics. For example, if w_1 has a frequency that is very close to the natural frequency of x_2 and, coincidentally, x_2 has a small damping, the disturbance could easily excite the hidden states and even cause instability.

Remark 2: Equation (1) only gives a basic form of the systems we consider and its applicability can be further extended.

1) The hidden dynamics may also have a control input u_2, i.e., $\dot{x}_2 = f_2(x_1, x_2, u_1, u_2)$. In this case one could argue that the effect of w_1 on x_2 can be eliminated by u_2. In practice, however, difficulty may occur due to physical limits of the feasible control input u_2.
2) The variable u_1 in (1) can be either a direct or indirect control input. Here, indirect control input means that it is not the input of the final actuator, but an intermediate control variable yielded by specific control scheme, the virtual control variable in a back-stepping scheme, for example.

Remark 3: Natural frequency of a state indicates how fast the state may change during a dynamic process under constraints of system dynamics and other boundary conditions. Assumption 1 is not uncommon in practice, which is termed as time-scale separation [27], the time scale differences among acceleration, velocity, and position in a motion control system, for example. This assumption gives a frequency domain interpretation of the situation that some disturbances may only affect part of system dynamics significantly, as indicated in Remark 1.

Remark 4: It could be argued that feasible control band of u_1 may be much lower than the disturbance frequency, thus the effect of w_1 is suppressed by available control input. However, one cannot predict whether the feasible control band is close to that of specific disturbance. As demonstrated by the example given in Section IV, the bandwidth of the aerodynamic actuator does stay close to the frequencies of the disturbance and the hidden modes.

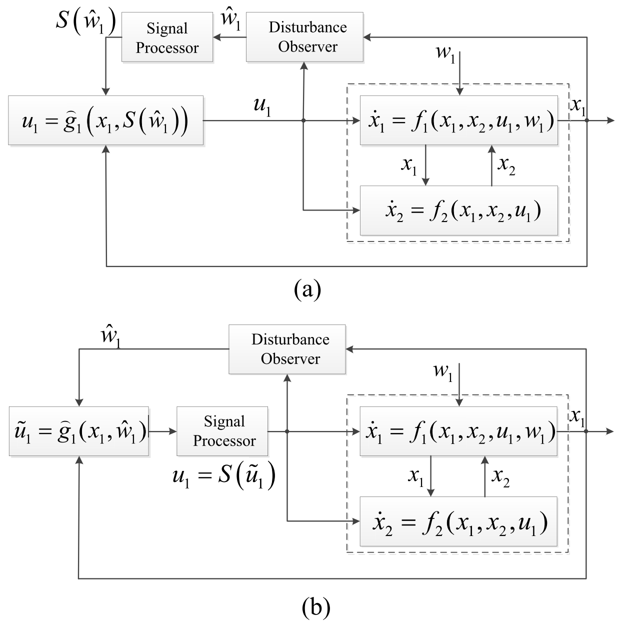

Fig. 3. System diagram for the closed-loop system with CDN. (a) System structure with CDN in the form of (4). (b) System structure with CDN in the form of (5).

The above analyses tell that full compensation, which is intended to improve system performance, *may* have side effect and degrade system performance. We cautiously use the word "may" because it depends on the deep characteristic analysis of specific plant to be controlled. A possible solution to eliminate this potential drawback is to construct CDN, in contrast with conventional full compensation.

C. Conditional Disturbance Negation

For (1), we define CDN as a disturbance negation principle that generates the following formalized control law:

$$u_1 = \widehat{g}_1\left(x_1, S(\hat{w}_1)\right) \tag{4}$$

or

$$u_1 = S\Big(\widehat{g}_1\left(x_1, \hat{w}_1\right)\Big) \tag{5}$$

where $S(\cdot)$ is a signal processor that is designed according to characteristics of the disturbance and system dynamics. The difference between (4) and (5) lies in that the signal processor is put following the observer in (4) and behind the feedback controller in (5), with the structure depicted as Fig. 3(a) and (b), respectively. The core idea is that CDN evaluates and processes the estimated information ($\hat{w}_1$) first, and then selectively feeds the processed information according to characteristics of the disturbance and system dynamics for control law synthesis. In this sense, CDN does not *do* disturbance negation directly according to what the observer *sees* as in (3), but *thinks* before taking actions. This thinking step includes trying to figure out what the estimated information is, how its quality is, and how to use it more wisely. Therefore, CDN contains the signal processor $S(\cdot)$ to conditionally restrict the use of observer-based negation.

Equations (4) and (5) represent a formalized design without specific mathematical description because CDN is proposed as a general design principle for either linear or nonlinear systems, regardless of specific feedback controller, observer, or signal processor design methods. Although CDN still contains a two-degree-of-freedom configuration, including a controller and a DOB which is widely termed as disturbance "compensation" or "cancelation" in current literatures, here we carefully choose the term "negation" based on the following *linguistic* consideration.

1) Negation is adopted to emphasize an active operation to directly obtain the disturbance information and suppress it, while compensation seems to represent a passive solution where control action is actuated only after the disturbance has already caused some effects on a system.
2) CDN does not seek to reject all disturbances, but those that have impacts on the control processes we care about. In this sense, our objective is not to "cancel" all disturbances, but to stop them from having impacts on specific control process.

Note that we use the term compensation to denote the observer-based disturbance rejection method hereinbefore. For better expression, hereafter we use the term negation instead. Accordingly, compared to CDN, the conventional full compensation scheme shown in Fig. 2 is termed as full disturbance negation (FDN) hereafter. A generalized CDN design process for (4) can be summarized as follows.

Step 1: Construct a DOB using any observer design method, such as DOB [8] or extended state observer (ESO) [6], to obtain the estimate $\hat{w}_1$of the disturbance.

Step 2: Design a signal processor $S(\hat{w}_1)$ to conditionally feed the estimated value $\hat{w}_1$ for control law synthesis based on deep system characteristics analysis.

Step 3: Synthesize a feedback control law $u_1 = \widehat{g}_1 (x_1, S(\hat{w}_1))$ using the processed estimated disturbance.

Such a generalized process for (5) can be similarly obtained. It is desirable that we give a general design method for $S(\cdot)$. Unfortunately, it is not feasible for diverse systems. A general guideline is to inspect potential drawbacks of FDN by deep system analysis.

Remark 5: CDN is proposed as a general design principle, hence system (1) can be extended to an even more general system

$$\begin{cases} \dot{x} = f(x, u, d) \\ y = h(x) \end{cases} \tag{6}$$

where $x \in \mathbb{R}^n$, $u \in \mathbb{R}^m$, $d \in \mathbb{R}^p$, and $y \in \mathbb{R}^q$are the state, the control input, the total disturbance (including internal uncertainty and external disturbance), and the output vectors, respectively. f and h are adequate functions representing the state and output dynamics of the system. Assume the disturbance d is estimated by an observer with its estimated value $\hat{d}$, then the control law under CDN principle can be designed as $u = F(x, S(\hat{d}))$ or $u = S(F(x, \hat{d}))$, where $F(\cdot)$ is a proper feedback controller. System (1) is a special example of (6). In this sense, although the side effect of observer-based robust control has already been discussed through the famous compliant mechanical systems and resonance ratio control (RRC) technique [18], [19], we contribute another typical example that reveals the side effect of FDN through a severe cross-coupling perspective. Actually, it can be derived that RRC in [18] and [19] is a special signal processor in the CDN frame where the signal processor is designed to recover the canceled reaction torque disturbance information with an adjustable feedback gain. CDN offers a flexible and effective approach to the signal processor design. Other potential implementation methods include direct notch filtering (which is adopted in the examples of Sections III and IV), disturbance characterization indicator-based method [22], optimal control with frequency weighting within the cost function [28], and frequency shaping method [29].

Next, we will separately study an LTI case and a nonlinear case to exemplify the analysis and control design under CDN principle. An additional difference between these two cases lies in that there is only control input coupling in the first case, while state couplings are also considered in the second example, yielding a comprehensive demonstration of (1).

III. Linear Time-Invariant Numerical Case Study

For the LTI case, we take the transient function approach for quantitative study. Consider the plant

$$\begin{cases} y_1 = G_{1p}(s) \cdot G_{2p}(s) \cdot u_1 + G_{2p}(s) \cdot w_1 \\ y_2 = G_{3p}(s) \cdot u_1. \end{cases} \tag{7}$$

This is a linear example of (1), with only control input coupling considered. $G_{1p}(s)$ together with $G_{2p}(s)$ describes the first subsystem, and $G_{3p}(s)$describes the second subsystem, i.e., the hidden system dynamics. For simplicity, consider both subsystems as single-input–single-output (SISO) systems, with the outputs separately denoted as y_1 and y_2. Our control objective is to let y_1 track its reference command r_1 in the presence of disturbance w_1, and keep the hidden subsystem well behaved. Without loss of generality, here the plant of the first subsystem is taken as $G_{1p}(s) \cdot G_{2p}(s)$, indicating that the disturbance w_1 only acts on part of the plant dynamics directly. Similar assumptions to Assumptions 1 and 2 also hold for (7).

Next, we will separately design a generic feedback scheme with no disturbance negation (NDN) and a FDN scheme for (7). Comparison of these two schemes naturally leads to the design of a CDN scheme.

A. Generic Feedback With No Disturbance Negation

Consider a feedback control scheme without disturbance negation as Fig. 4, where $G_c(s)$ is a proper feedback controller that stabilizes the y_1 subsystem. The transfer function from the reference command to the first output is

$$\frac{y_1}{r_1} = \frac{G_c(s)G_{1p}(s)G_{2p}(s)}{1 + G_c(s)G_{1p}(s)G_{2p}(s)}. \tag{8}$$

The transfer functions from the disturbance to the two subsystem outputs can be separately given as

$$\frac{y_1}{w_1} = \frac{G_{2p}(s)}{1 + G_c(s)G_{1p}(s)G_{2p}(s)} \tag{9}$$

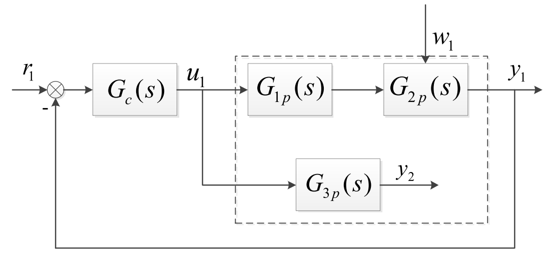

Fig. 4. System diagram without disturbance negation.

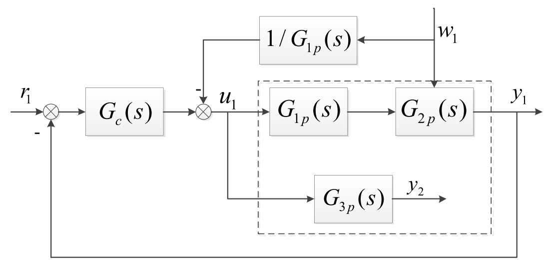

Fig. 5. System diagram with FDN.

and

$$\frac{y_2}{w_1} = -\frac{G_c(s)G_{2p}(s)G_{3p}(s)}{1 + G_c(s)G_{1p}(s)G_{2p}(s)}. \tag{10}$$

For a special case where the first subsystem plant can be completely represented by $G_{2p}(s)$, we simply set $G_{1p}(s) = 1$ for (8)–(10).

B. Full Disturbance Negation

Now, consider an FDN control scheme. Suppose that the observer can estimate the disturbance "perfectly," i.e., the estimated value exactly matches the actual disturbance. Therefore, the disturbance can be supposed as measurable. This assumption is not practical but convenient for a unified derivation because we do not need to consider specific observation error. The closed-loop system with FDN can be depicted as Fig. 5. Here, the negator is explicitly represented as $-1/G_{1p}(s)$ such that $G_c(s)$ is designed merely as a nominal input–output tracking controller.

Accordingly, the transfer function from the reference command to the first output is the same as (8), and the transfer functions from the disturbance to the two subsystem outputs can be separately given as

$$\frac{y_1}{w_1} = 0 \tag{11}$$

and

$$\frac{y_2}{w_1} = \frac{-G_{3p}(s)}{G_{1p}(s)}. \tag{12}$$

Equation (11) indicates that the disturbance has no effect on the first output, which means the negator completely cancels the disturbance as intended. Again, if the first subsystem plant can be completely represented by $G_{2p}(s)$, i.e., $G_{1p}(s) = 1$, the transfer function (12) is simply $-G_{3p}(s)$. This means that the disturbance is directly fed to the hidden subsystem due to the negator.

Now, we start to compare the two schemes. Recall Assumption 2 that tells w_1 has negligible impact on y_1, which means $G_{2p}(s) \cdot w_1 \approx 0$. Thus, (9) is approximately equivalent to (11). Moreover, the impact on y_2 of w_1 may also be small in view of (10). That means the observer-based negation contributes little performance improvement. As a cost, however, for (12) if $G_{1p}(s) = 1$, w_1 is directly fed to the hidden subsystem and may degrade its performance; if $G_{1p}(s) \neq 1$, a worse case lies in that $G_{1p}(s)$ has right-half plane (RHP) zeros, which makes (12) unstable and yields an even worse performance of the hidden subsystem.

For numerical demonstration, take the plant as

$$G_{1p} = 1,\, G_{2p} = \frac{\omega_{n1}^2}{s^2 + 2\zeta_1\omega_{n1}s + \omega_{n1}^2}$$
$$G_{3p} = \frac{\omega_{n2}^2}{s^2 + 2\zeta_2\omega_{n2}s + \omega_{n2}^2} \tag{13}$$

with $\zeta_1 = 1$, $\omega_{n1} = 1$ rad/sec, $\zeta_2 = 0.02$, and $\omega_{n2} = 10$ rad/sec. This example indicates that: 1) the hidden subsystem has weak stability with a small damping ratio and 2) natural frequencies of the two subsystems are far separated (ten times difference here), as indicated by Assumption 1. Since specific control algorithm is not cared about in this article, we trivially design $G_c(s)$ as a PID controller

$$G_c(s) = k_p + k_i/s + k_d s. \tag{14}$$

The transfer functions (8)–(10) are obtained as

$$\frac{y_1}{r_1} = \frac{k_d s^2 + k_p s + k_i}{s^3 + (k_d + 2)s^2 + \big(k_p + 1\big)s + k_i} \tag{15}$$
$$\frac{y_1}{w_1} = \frac{s}{s^3 + (k_d + 2)s^2 + \big(k_p + 1\big)s + k_i} \tag{16}$$
$$\frac{y_2}{w_1} = -\frac{k_d s^2 + k_p s + k_i}{s^3 + (k_d + 2)s^2 + \big(k_p + 1\big)s + k_i} \times \frac{\omega_{n2}^2}{s^2 + 2\zeta_2\omega_{n2}s + \omega_{n2}^2}. \tag{17}$$

Simply using Routh stability criterion and choosing the controller parameters

$$\begin{cases} k_p + 1 > 0,\, k_i > 0,\, k_d + 2 > 0 \\ \big(k_p + 1\big)(k_d + 2) - k_i > 0 \end{cases} \tag{18}$$

can guarantee the stability of the y_1 subsystem. We trivially choose $k_p = 2$, $k_i = 1$, and $k_d = 0.5$. Bode diagrams of (16) and (17) are given as Fig. 6(a) and (b), respectively. As expected, y_2 is much more sensitive than y_1 to high-frequency disturbance which has the frequency close to the natural frequency of G_{3p}, but the magnitude is almost below zero.

On the contrary, if an observer is integrated as Fig. 5, Bode diagram of (12) is given as Fig. 7. In this case, y_2 may be greatly affected by a disturbance which has the frequency close to 10 rad/s.

C. Conditional Disturbance Negation

Based on the scheme of FDN, a signal processor, denoted as $G_N(s)$, is integrated, yielding a CDN scheme as depicted in Fig. 8. Accordingly, we have

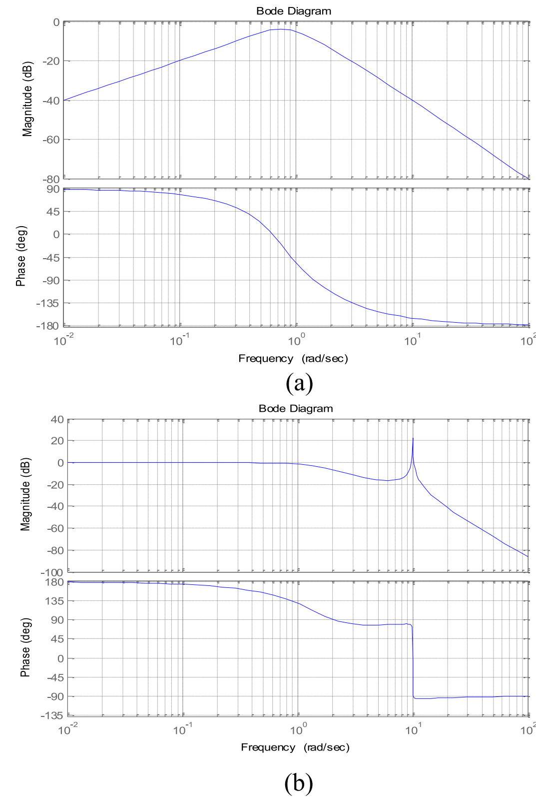

Fig. 6. Bode diagrams of the transfer function from the disturbance to: (a) y_1 and (b) y_2 with NDN.

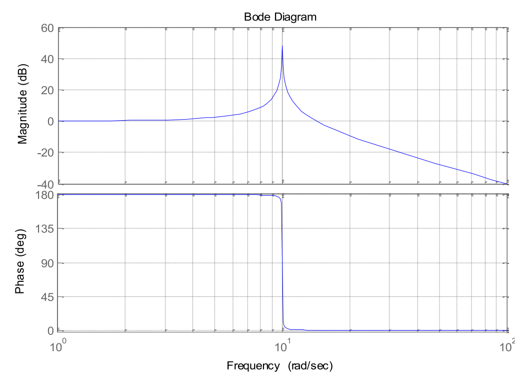

Fig. 7. Bode diagrams of the transfer function from the disturbance to y_2 with FDN.

$$\frac{y_1}{r_1} = \frac{G_c(s)G_N(s)G_{1p}(s)G_{2p}(s)}{1 + G_c(s)G_N(s)G_{1p}(s)G_{2p}(s)} \tag{19}$$
$$\frac{y_1}{w_1} = \frac{G_{2p}(s)(1 - G_N(s))}{1 + G_c(s)G_N(s)G_{1p}(s)G_{2p}(s)} \tag{20}$$
$$\frac{y_2}{w_1} = -\frac{y_1}{w_1}G_c(s)G_N(s)G_{3p}(s) - \frac{G_N(s)G_{3p}(s)}{G_{1p}(s)}. \tag{21}$$

For demonstration, design the signal processor as a notch filter

$$G_N(s) = \frac{s^2 + \omega_N^2}{s^2 + \omega_N s/Q_N + \omega_N^2} \tag{22}$$

with $\omega_N = \omega_{n2}$ and $Q_N = 1$. Intuitively, since the natural frequency of $G_{2p}(s)$ is much smaller than the frequency of w_1

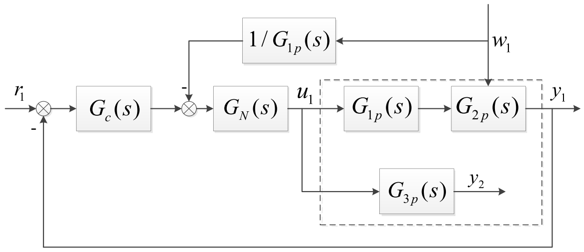

Fig. 8. System diagram with CDN.

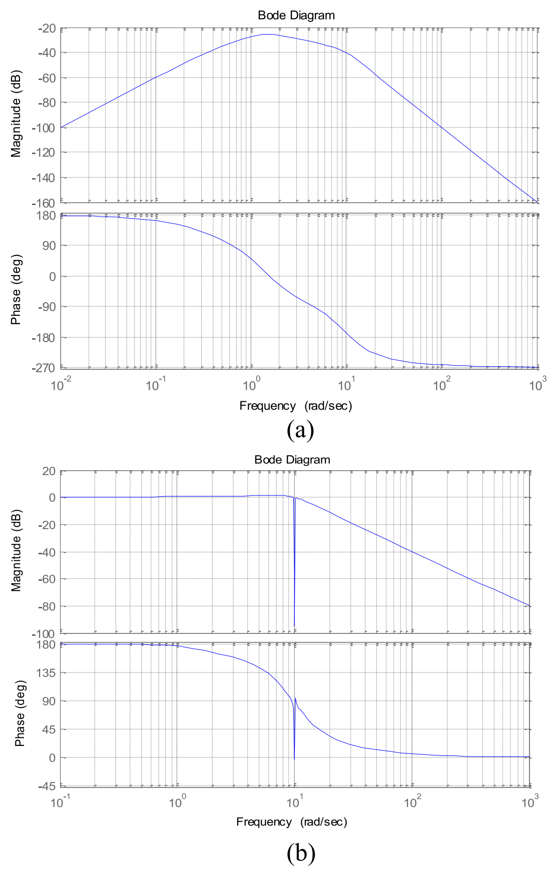

Fig. 9. Bode diagrams of the transfer function from the disturbance to: (a) y_1 and (b) y_2 with CDN.

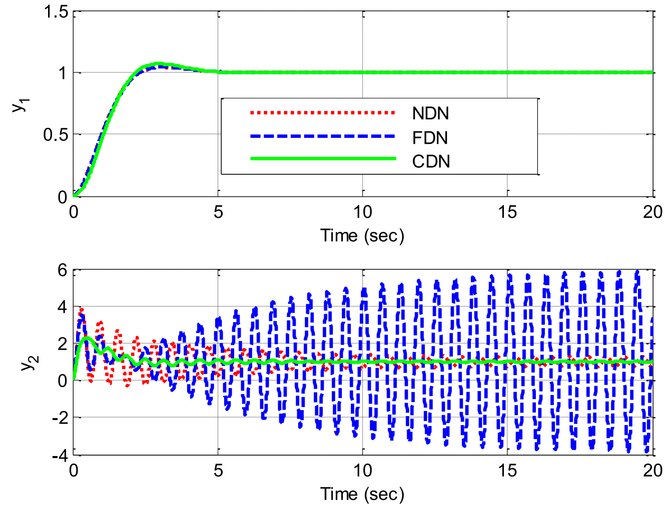

Fig. 10. Simulation results of the linear example.

and y_1/w_1 should be quite small. Then the first item in (21) can be ignored and $y_2/w_1 \approx -G_N(s)G_{3p}(s)/G_{1p}(s)$. Compared with (12) where $y_2/w_1 = -G_{3p}(s)/G_{1p}(s)$, it is obvious that the notch filter is added to suppress the influence of w_1. These intuitive analyses are supported by the Bode diagrams of (20) and (21) as Fig. 9. As expected, y_1 is robust to the disturbance. More importantly, compared to Fig. 7, y_2 also exhibits better disturbance rejection ability.

Next, we give a comparison in the time domain. Suppose there exists a disturbance $w_1 = 0.2\sin(\omega_{n2}t)$, that is, the frequency of the disturbance signal is the same as the natural frequency of $G_{3p}(s)$. The reference command is given as $r_1 = 1$. The simulation results with the NDN, FDN, and CDN control schemes are compared in Fig. 10. In all schemes y_1 can track the reference command well, but the responses of y_2 are quite different. Without negation the response of y_2 can be kept in a relatively small magnitude; with FDN, however, it is excited by the disturbance and oscillation with a large magnitude occurs; with CDN, the oscillation is well suppressed, better than NDN. This indicates that an appropriate CDN scheme has little impact on normal (y_1) subsystem performance but can protect hidden (y_2) subsystem from being excited by some disturbances.

To summarize, the control laws for (7) with NDN, FDN, and CDN, as counterparts of (2), (3), and (5), are, respectively, listed as

$$u_1 = G_c(s) \cdot e_{y_1} \tag{23}$$

$$u_1 = G_c(s) \cdot e_{y_1} - \frac{1}{G_{1p}(s)} w_1 \tag{24}$$

and

$$u_1 = G_N(s) \cdot \left[G_c(s) \cdot e_{y_1} - \frac{1}{G_{1p}(s)} w_1 \right] \tag{25}$$

where $e_{y_1} = r_1 - y_1$is the tracking error of y_1. Obviously the signal processor in CDN is taken as the form of (5)

$$S\left(\widehat{g}\ (s)\right) = G_N(s) \cdot \widehat{g}\ (s) \tag{26}$$

where

$$\widehat{g}\ (s) = G_c(s) \cdot e_{y_1} - \frac{1}{G_{1p}(s)} w_1$$

and $G_N(s)$ is the notch filter (22).

One may argue that the example given in this section is too particular because we know exactly the natural frequencies of both subsystems and we add a specific disturbance that has great impact on one subsystem while almost has no impact on the other. Next, we will give a more complex case to exemplify that it is not uncommon in practice, and it is of great importance to dig system characteristics as much as possible before control design.

IV. Nonlinear FAHV Case Study

In this section, we will exemplify the effectiveness of CDN in control design for an FAHV [30]. A back-stepping control scheme was constructed in [20] and [21]. As specific control method is not what we care about in this article, we primarily analyze how FDN causes side effects and why CDN is necessary. Backgrounds and detailed control design can be referred to [20] and [21].

A. Model Description

Disturbed motion equations of FAHV altitude system are described as

$$\dot{h} = V \sin\gamma + w_h \tag{27}$$
$$\dot{\gamma} = (L + T\sin\alpha)/(mV) - g\cos\gamma/V + w_\gamma \tag{28}$$
$$\dot{\alpha} = Q - \dot{\gamma} + w_\alpha \tag{29}$$
$$\dot{Q} = M/I_{yy} + w_Q \tag{30}$$
$$\ddot{\eta}_i = -2\xi_i\omega_i\dot{\eta}_i - \omega_i^2\eta_i + N_i, \quad i = 1, 2, 3. \tag{31}$$

Here, h, γ, α, and Q are four rigid states, representing altitude, flight-path angle (FPA), angle of attack (AOA), pitch rate, respectively, and w_h, w_γ, w_α, and w_Q denote external disturbances in these four channels. η_i and $\dot{\eta}_i$ are the first three flexible modes and their derivatives, with modal frequencies $\omega_1 = 21.17$ rad/s, $\omega_2 = 53.92$ rad/s, and $\omega_3 = 109.1$ rad/s. All flexible modes have the damping ratio $\xi_i = 0.02$, indicating a severe mode vibration. The flexible modes describe how the vehicle may blend in hypersonic flight due to its long, slender fuselage with light materials. However, these flexible states are difficult to be measured. Note that all rigid and flexible modal frequencies are characterized at a trimmed condition given in [30] where the nonlinear model is linearized for frequency domain analysis. Other symbols involve vehicle velocity V, mass m, longitudinal moment of inertia I_{yy}, and gravitational acceleration g. The control input to be designed is the elevator deflection δ_e. The aerodynamic lift L, drag D, pitching moment M, thrust T, and generalized flexible forces N_i are significantly coupled with the flight states and control inputs. Their detailed expressions are given in [21] but can be written into the following formalized expressions:

$$\begin{cases} L = f_L(\alpha, \eta, \delta_e) \\ D = f_D(\alpha, \eta, \delta_e) \\ M = f_M(\alpha, \eta, \delta_e) \\ T = f_T(\alpha, \eta) \\ N_i = f_{N_i}(\alpha, \eta, \delta_e), \quad i = 1, 2, 3 \end{cases} \tag{32}$$

to emphasize the key independent variables, with $\eta = [\eta_1, \eta_2, \eta_3]^T$.

It is seen that all forces and the pitching moment that determine the rigid dynamics are affected by the flexible modes η, and inversely, the generalized flexible forces N_i are also affected by the rigid modes, especially, the AOA α. Moreover, all rigid and flexible modes are explicitly affected by control input δ_e. Hence, couplings exist among both rigid/flexible states and control input, resulting in a quite complex version of the general system (1). Denoting $x_1 = [h, \gamma, \alpha, Q]^T$ as the rigid modes, $x_2 = [\eta^T, \dot{\eta}^T]^T$ as the flexible modes, $u_1 = \delta_e$ as the control input, and $w_1 = [w_h, w_\gamma, w_\alpha, w_Q]^T$ as the disturbances, we can rewrite system (27)–(31) as

$$\begin{cases} \dot{x}_1 = f_{\text{rigid}}(x_1, x_2, u_1, w_1) \\ \dot{x}_2 = f_{\text{flexible}}(x_1, x_2, u_1) \end{cases} \tag{33}$$

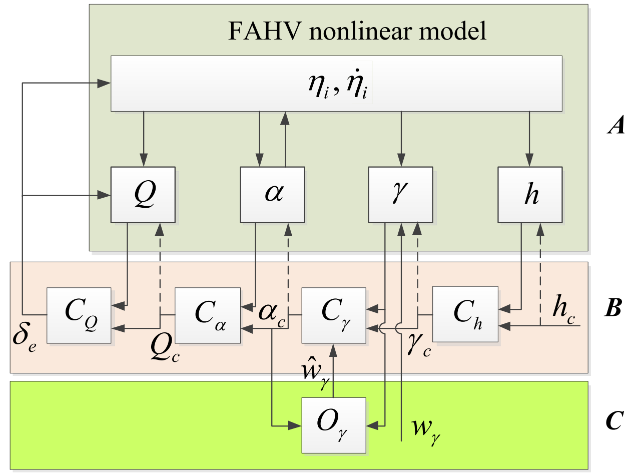

Fig. 11. Overall logic of the altitude control with FDN.

where f_{rigid} and f_{flexible} can be directly derived from (27)–(31) and detailed expressions of the forces and moment. Therefore, this is exactly an example of the general system (1). Natural frequency of the slowest flexible mode η_1 is almost 5–10 times of the fastest rigid mode Q [30], so there is indeed a large time-scale separation between x_1 and x_2, which means Assumption 1 holds. Our control objective is to let the altitude h track its reference command, while keep the flexible modes from being significantly excited.

B. Full Disturbance Negation

In [20] and [21] a back-stepping scheme with FDN was adopted which decomposed the altitude control into four first-order cascaded subsystems, each incorporating a nonlinear dynamic inversion [31]-based nominal controller and an ESO [6]-based negator. By ignoring some tedious details, the overall control logic can be illustrated as Fig. 11. It is explained as follows.

Part A: The FAHV nonlinear model. It consists of four rigid states: the altitude h, FPA γ, AOA α, and pitch rate Q, each block representing a first-order rigid dynamics listed as (27)–(30). It also consists of six flexible modes η_i and $\dot{\eta}_i$, of which the dynamics are modeled as (31). Couplings among the rigid and flexible modes through the forces and moment (32) are also illustrated by the arrowed lines.

Part B: The nominal control scheme. With proper assumptions, (27)–(30) can be rewritten into a strict-feedback form as [21]

$$\dot{h} = f_h + g_h\gamma + d_h \tag{34}$$
$$\dot{\gamma} = f_\gamma + g_\gamma\alpha + d_\gamma \tag{35}$$
$$\dot{\alpha} = f_\alpha + g_\alpha Q + d_\alpha \tag{36}$$
$$\dot{Q} = f_Q + g_Q\delta_e + d_Q \tag{37}$$

where d_j are lumped disturbances consisting of w_j and other modeling errors, and details of d_j, f_j, and g_j can be found in [21], $j = h, \gamma, \alpha, Q$. Then a back-stepping framework with four cascaded nominal controllers is constructed, each for a rigid dynamics. A former controller generates a reference command for the subsequent dynamics. For example, C_γ

generates a reference command α_c for the AOA to follow. If the subsequent controller C_α works normally, the actual AOA α should track α_c well. Therefore, we use the dashed lines to indicate that the reference commands can determine the actual flight states implicitly.

For demonstration, we consider the FPA dynamics only in this article. A nominal FPA controller without disturbance compensation is designed as

$$\bar{\alpha}_c = \left(-k_\gamma e_\gamma - f_\gamma + \dot{\gamma}_c\right)/g_\gamma \tag{38}$$

where $e_\gamma = \gamma - \gamma_c$ is the tracking error of FPA, and k_γ is a proper controller gain.

Part C: The observer-based negation. ESOs $O_j, j = h, \gamma, \alpha, Q$, are combined with the nominal controllers, also each for a rigid mode dynamics. For the disturbed FPA model (35), the modeling error is verified to be negligible, thus we denote $d_\gamma = w_\gamma$. An ESO is designed as

$$\begin{cases} \hat{e}_\gamma = \hat{\gamma} - \gamma \\ \dot{\hat{\gamma}} = f_\gamma + g_\gamma \alpha_c + \hat{w}_\gamma - \beta_{\gamma 1}\hat{e}_\gamma \\ \dot{\hat{w}}_\gamma = -\beta_{\gamma 2}\tilde{e}_\gamma \end{cases} \tag{39}$$

where $\hat{\gamma}$ and $\hat{w}_\gamma$ are the estimates of γ and w_γ, $\hat{e}_\gamma$ is the estimation error, and $\beta_{\gamma 1}$ and $\beta_{\gamma 2}$ are proper observer gains. Then $\hat{w}_\gamma$ is fed for negation, yielding the final FDN control law as

$$\alpha_c = \bar{\alpha}_c - \hat{w}_\gamma / g_\gamma. \tag{40}$$

Now, we analyze potential drawback of this observer-based negation scheme in Fig. 11. Assume the disturbance w_γ is perfectly estimated as $\hat{w}_\gamma$, then the control variable α_c, as revealed in (40), will contain a negation component that is directly related to w_γ. This negation component can be reflected by both the rigid state α and the final actuator control input δ_e, both of which have great impacts on the flexile modes through the generalized flexible forces N_i. Now, suppose w_γ contains a signal component that has a frequency close to the natural frequencies of the flexible modes, these modes may be excited by the negation component. In return, the excited flexible modes will react on the rigid modes, which may make the cross-coupling much worse. Finally, the overall system may become unstable.

C. Conditional Disturbance Negation

CDN can protect the flexible modes from being excited. A direct solution is to add a notch filter behind the observer. Still take the FPA dynamics for demonstration. The CDN scheme is shown in Fig. 12. The notch filter N_γ is designed such that normal estimated signals are passed through for disturbance rejection in the FPA dynamics, while the signals that may excite the flexible modes are suppressed. Therefore, N_γ can take the same form as (22), with $\omega_N = 21$ rad/s and $Q_N = 0.5$. Ideally, there should be three notch filters for the first three flexible modes, respectively. However, because the first mode η_1 has much greater impact than the other two flexible modes in practice [32], and also because frequencies of the latter two modes are much higher than the rigid modes, which makes their couplings to rigid dynamics much weaker,

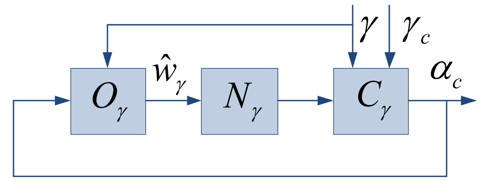

Fig. 12. CDN for the FPA dynamics.

we only consider the first mode suppression here. The central frequency ω_N is selected around ω_1, the natural frequency of the first flexible mode, but not necessarily exactly the same to indicate a frequency uncertainty.

Again, we summarize that the control law for the FPA dynamics with FDN is in (40), while the one with CDN is

$$\alpha_c = \bar{\alpha}_c - S\left(\hat{w}_\gamma\right)/g_\gamma. \tag{41}$$

The signal processor in CDN is taken as the form of (4) where

$$S\left(\hat{w}_\gamma\right) = N_\gamma \cdot \hat{w}_\gamma. \tag{42}$$

D. Simulation Comparison

We finally conduct a simulation comparison to demonstrate the superiority of CDN. Reference commands are given such that the vehicle climbs and accelerates from an initial trimmed condition (altitude 85 000 ft, velocity 7846.4 ft/s) to the altitude 110 000 ft and the velocity 10 500 ft/s. Basic control parameters are set as those in [20]. Assume two external disturbances are added to the FPA dynamics (28): a low-frequency disturbance $w_{\gamma 1} = 0.001\sin(0.5t)$ and a high-frequency disturbance $w_{\gamma 2} = 0.005\sin(21t)$ during the period $t = 400 \sim 500$ s. Other disturbances and uncertainties include 40% parameter uncertainty added to the rigid forces and moment during $t = 0 \sim 400$ s, and the flexibility contribution to the rigid dynamics in the entire flight. All of these disturbances and uncertainties constitute the total disturbance w_γ to the FPA dynamics. Therefore, w_γ contains both low- and high- frequency components. Particularly, the high-frequency component $w_{\gamma 2}$ has a frequency that is very close to the natural frequency of the first flexible mode η_1. We take three control schemes that are separately with NDN, FDN, and CDN for comparison. The simulation results are depicted in Fig. 13. It is seen from Fig. 13(a) that both NDN and CDN schemes can stabilize the altitude dynamics, but the latter gives a better response as indicated by the tracking error shown in Fig. 13(b). This comparison indicates the necessity of observer-based negation. However, the FDN makes the altitude diverge after the disturbance $w_{\gamma 2}$ is added, as shown in Fig. 13(a). This is because the high-frequency disturbance excites the flexible modes as shown in Fig. 13(d), and in return, these excited modes degrade rigid response. CDN, however, succeeds in protecting the flexible modes from being severely excited, as shown in Fig. 13(c). The original estimated disturbance is plotted in Fig. 13(e), indicating clearly that all disturbances are well estimated. However, as shown in Fig. 13(f), the high-frequency signal during $t = 400 \sim 500$ s is suppressed by the notch filter. This means the estimated disturbances are selectively adopted for negation.

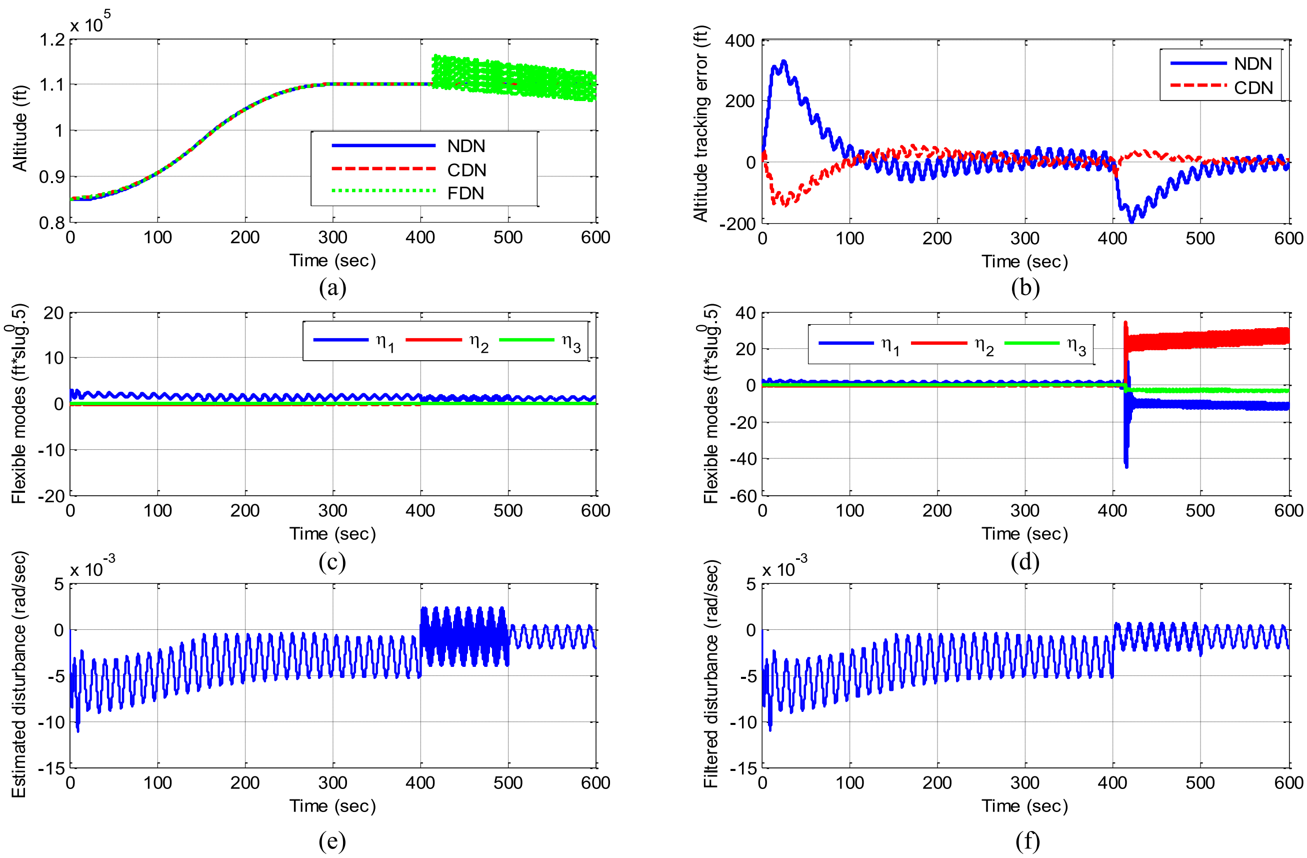

Fig. 13. Simulation results of the nonlinear FAHV example. (a) Altitude responses in NDN, CDN, and FDN schemes. (b) Altitude tracking errors in NDN and CDN schemes. (c) Flexible modes in CDN scheme. (d) Flexible modes in FDN scheme. (e) Original estimated disturbance in CDN scheme. (f) Filtered estimated disturbance in CDN scheme.

Remark 6: This example indicates clearly that CDN makes a proper tradeoff between normal disturbance rejection and hidden state suppression. That means we do not blindly seek for the performance of disturbance rejection. On the contrary, we should have an overall evaluation of multiple (maybe conflicting) design requirements by deep analysis of system characteristics.

Remark 7: The flexible modal frequency and damping ratio may change during hypersonic flight due to fuel consumption, payload variation, or atmospheric heating. In this case, a deep understanding of vehicle characteristics is of significance, which can give a guideline to design an online frequency estimator [33] so that the notch filter can adaptively track practical flexible modal frequency.

V. Conclusion

Although limits and potential drawbacks of conventional DOB-based control have been discussed, we provide another typical example through a class of cross-coupling systems in this article. More importantly, the design principle of CDN is proposed for systems suffering from the side effects of conventional observer-based compensation. We give a basic description of the cross-coupling system and conduct qualitative analysis to discuss why FDN may cause side effects and how CDN works. A numerical LTI example and a more complex nonlinear FAHV example follow, exhibiting more quantitative analysis and simulation results to demonstrate the effectiveness of CDN. Frequency domain languages seem to be a straightforward tool for analysis and synthesis of such systems.

As an initial attempt, our purpose is not to present specific methods for control design, but to point out the necessity of CDN. It raises an interesting question on how to use an observer more wisely according to system characteristics. The proposed work also arouses our awareness of the importance of signal processing, rather than control algorithm design, in engineering practice, which constructs an information-centric control concept that has not been well understood yet. In the future work, more implementation methods for the signal processor should be developed. A promising direction is to draw lessons from the information science, the abundant data-driven-based methods, for example.

References

[1] Z. Gao, "On the problem of information in engineering cybernetics," *J. Sys. Sci. Math. Sci.*, vol. 36, no. 7, pp. 908–923, 2016.

[2] Z. Gao, "On the centrality of disturbance rejection in automatic control," *ISA Trans.*, vol. 53, no. 4, pp. 850–857, Jul. 2014.

[3] R. Brockett, "New issues in the mathematics of control," in *Mathematics Unlimited—2001 and Beyond*. Berlin Heidelberg, Germany: Springer, 2001, pp. 189–220.

[4] J. Preminger and J. Rootenberg, "Some considerations relating to control systems employing the invariance principle," *IEEE Trans. Autom. Control*, vol. AC-9, no. 3, pp. 209–215, Jul. 1964.

[5] J. Han, "From PID to active disturbance rejection control," *IEEE Trans. Ind. Electron.*, vol. 56, no. 3, pp. 900–906, Mar. 2009.

[6] Q. Zheng, L. Dong, D. H. Lee, and Z. Gao, “Active disturbance rejection control for MEMS gyroscopes,” *IEEE Trans. Control Syst. Technol.*, vol. 17, no. 6, pp. 1432–1438, Nov. 2009.

[7] L. Zhao, Q. Li, B. Liu, and H. Cheng, “Trajectory tracking control of a one degree of freedom manipulator based on a switched sliding mode controller with a novel extended state observer framework,” *IEEE Trans. Syst., Man, Cybern., Syst.*, vol. 49, no. 6, pp. 1110–1118, Jun. 2019.

[8] W.-H. Chen, J. Yang, L. Guo, and S. Li, “Disturbance-observer-based control and related methods—An overview,” *IEEE Trans. Ind. Electron.*, vol. 63, no. 2, pp. 1083–1095, Feb. 2016.

[9] E. Sariyildiz and K. Ohnishi, “A guide to design disturbance observer,” *J. Dyn. Syst. Meas. Control*, vol. 136, no. 2, pp. 1–10, Mar. 2014.

[10] H. K. Khalil, “Extended high-gain observers as disturbance estimators,” *SICE J. Control Meas. Syst. Integr.*, vol. 10, no. 3, pp. 125–134, May 2017.

[11] B. Xu, F. Sun, Y. Pan, and B. Chen, “Disturbance observer based composite learning fuzzy control of nonlinear systems with unknown dead zone,” *IEEE Trans. Syst., Man, Cybern., Syst.*, vol. 47, no. 8, pp. 1854–1862, Aug. 2017.

[12] D. Qian, H. Ding, S. Lee, and H. Bae, “Suppression of chaotic behaviors in a complex biological system by disturbance observer-based derivative-integral terminal sliding mode,” *IEEE/CAA J. Automatica Sinica*, vol. 7, no. 1, pp. 126–135, Jan. 2020.

[13] E. Sariyildiz and K. Ohnishi, “Stability and robustness of disturbance-observer-based motion control systems,” *IEEE Trans. Ind. Electron.*, vol. 62, no. 1, pp. 414–422, Jan. 2015.

[14] Y. Liu, Y. Fu, W. He, and Q. Hui, “Modeling and observer-based vibration control of a flexible spacecraft with external disturbances,” *IEEE Trans. Ind. Electron.*, vol. 66, no. 11, pp. 8648–8658, Nov. 2019.

[15] G. Besançon, *Nonlinear observers and applications*. Berlin Heidelberg, Germany: Springer, 2007.

[16] Z. Pu, R. Yuan, J. Yi, and X. Tan, “A class of adaptive extended state observers for nonlinear disturbed systems,” *IEEE Trans. Ind. Electron.*, vol. 62, no. 9, pp. 5858–5869, Sep. 2015.

[17] Y. Liu, F. Guo, X. He, and Q. Hui, “Boundary control for an axially moving system with input restriction based on disturbance observers,” *IEEE Trans. Syst., Man, Cybern., Syst.*, vol. 49, no. 11, pp. 2242–2253, Nov. 2019.

[18] K. Yuki, T. Murakami, and K. Ohnishi, “Vibration control of 2 mass resonant system by resonance ratio control,” in *Proc. Int. Conf. IEEE Ind. Electron. Soc.*, 1993, pp. 2009–2014.

[19] S. Katsura and K. Ohnishi, “Force servoing by flexible manipulator based on resonance ratio control,” *IEEE Trans. Ind. Electron.*, vol. 54, no. 1, pp. 539–547, Feb. 2007.

[20] Z. Pu, R. Yuan, X. Tan, and J. Yi, “Active robust control of uncertainty and flexibility suppression for air-breathing hypersonic vehicles,” *Aerosp. Sci. Technol.*, vol. 42, pp. 429–441, Apr./May 2015.

[21] J. Sun, J. Yi, Z. Pu, and X. Tan, “Fixed-time sliding mode disturbance observer-based nonsmooth backstepping control for hypersonic vehicles,” *IEEE Trans. Syst., Man, Cybern., Syst.*, to be published.

[22] J. Sun, Z. Pu, and J. Yi, “Conditional disturbance negation based active disturbance rejection control for hypersonic vehicles,” *Control Eng. Pract.*, vol. 84, pp. 159–171, Mar. 2019.

[23] F. G. Shinskey, *Process Control Systems: Application, Design, and Adjustment*, 3rd ed. New York, NY, USA: McGraw-Hill, Sep. 1988.

[24] J.-H. She, M. Fang, Y. Ohyama, H. Hashimoto, and M. Wu, “Improving disturbance-rejection performance based on an equivalent-input-disturbance approach,” *IEEE Trans. Ind. Electron.*, vol. 55, no. 1, pp. 380–389, Jan. 2008.

[25] T. Umeno, T. Kaneko, and Y. Hori, “Robust servosystem design with two degrees of freedom and its application to novel motion control of robot manipulators,” *IEEE Trans. Ind. Electron.*, vol. 40, no. 5, pp. 473–485, Oct. 1993.

[26] L. Fagiano and C. Novara, “Learning a nonlinear controller from data: Theory, computation, and experimental results,” *IEEE Trans. Autom. Control*, vol. 61, no. 7, pp. 1854–1868, Jul. 2016.

[27] H. K. Khalil, *Nonlinear Systems*, 3rd ed. Upper Saddle River, NJ, USA: Prentice-Hall, 2002, pp. 610–625.

[28] L. A. Sievers and A. H. Flotow, “Linear control design for active vibration isolation of narrow band disturbances,” in *Proc. 27th Conf. Decis. Control*, Austin, TX, USA, 1988, pp. 1032–1037.

[29] Y. Chida, Y. Ishihara, T. Okina, T. Nishimura, K. Ohtomi, and R. Furukawa, “Identification and frequency shaping control of a vibration isolation system,” *Control Eng. Pract.*, vol. 16, no. 6, pp. 711–723, 2008.

[30] L. Fiorentini, A. Serrani, M. A. Bolender, and D. B. Doman, “Nonlinear robust adaptive control of flexible air-breathing hypersonic vehicles,” *J. Guid. Control Dyn.*, vol. 32, no. 2, pp. 401–416, Mar./Apr. 2009.

[31] M. Alam and S. Celikovsky, “On the internal stability of non-linear dynamic inversion: Application to flight control,” *IET Control Theory Appl.*, vol. 11, no. 12, pp. 1849–1861, Jul. 2017.

[32] J. Levin, P. A. Ioannou, and M. D. Mirmirani, “Adaptive mode suppression scheme for an aeroelastic airbreathing hypersonic cruise vehicle,” in *Proc. AIAA Guid. Navig. Control Conf. Exhibit*, Honolulu, HI, USA, Aug. 2008, Art. no. 2008–7137.

[33] L. Hsu, R. Ortega, and G. Damm, “A globally convergent frequency estimator,” *IEEE Trans. Autom. Control*, vol. 44, no. 4, pp. 698–713, Apr. 1999.

Zhiqiang Pu received the B.Eng. degree in automation control from Wuhan University, Wuhan, China, in 2009, and the Ph.D. degree in control theory and control engineering from the Institute of Automation, Chinese Academy of Sciences, Beijing, China, in 2014.

He is currently an Associate Professor with the Institute of Automation, Chinese Academy of Sciences, and also with the School of Artificial Intelligence, University of Chinese Academy of Sciences, Beijing. He has been supported by the Talent Program of Youth Innovation Promotion Association CAS since 2017. His research interests include nonlinear control, swarm robotics, and unmanned autonomous systems.

Jinlin Sun received the B.E. degree in automatic control from Jiangsu University, Zhenjiang, China, in 2016. He is currently pursuing the Ph. D. degree in robust adaptive control of hypersonic vehicles with the Institute of Automation, Chinese Academy of Sciences, Beijing, China, and also with the School of Artificial Intelligence, University of Chinese Academy of Sciences, Beijing.

His current research interests include robust control, flight control, and computational intelligence.

Jianqiang Yi (Senior Member, IEEE) received the B.Eng. degree in mechanical engineering from the Beijing Institute of Technology, Beijing, China, in 1985, and the M.Eng. and Ph.D. degrees in automation control from the Kyushu Institute of Technology, Kitakyushu, Japan, in 1989 and 1992, respectively.

From 1992 to 1994, he worked as a Research Fellow with the Computer Software Development Company, Tokyo, Japan. From 1994 to 2001, he was a Chief Engineer with MYCOM, Inc., Kyoto, Japan. Since 2001, he has been a Professor with the Institute of Automation, Chinese Academy of Sciences, Beijing. He is also currently with the School of Artificial Intelligence, University of Chinese Academy of Sciences, Beijing. His research interests include theories and engineering applications of intelligent control, adaptive control, intelligent robotics, and unmanned aerial vehicle systems.

Prof. Yi is an Associate Editor of the *Journal of Advanced Computational Intelligence and Intelligent Informatics* and *Journal of Innovative Computing, Information and Control*.

Zhiqiang Gao (Member, IEEE) received the Ph.D. degree in electrical engineering from the University of Notre Dame, Notre Dame, IN, USA, in 1990.

He has taught with Cleveland State University, Cleveland, OH, USA, ever since. Faced with ever widening chasm between control theory and practice, he returned to the roots of controls by collaborating extensively with engineers at NASA and industry in solving real-world problems, from which the foundation and authenticity of research were rebuilt. Collaborating with Prof. J. Han, he worked quietly on active disturbance rejection control for over 15 years, nurturing it from its early, conceptual stage to a maturing and emerging industrial control technology. In doing so, he made an obscure idea clear and established firmly a general design principle in dealing with uncertainties in industrial settings, often with staggering improvements in performance and energy saving. Asking basic, rudimentary question in research and in teaching, he and his team find creative solutions in practice and vitality in education. His research and teaching materials can be found at http://cact.csuohio.edu.